

Thermal expansion of LaAlO_3 and $(\text{La,Sr})(\text{Al,Ta})\text{O}_3$, substrate materials for superconducting thin-film device applications

B. C. Chakoumakos D. G. Schlom M. Urbanik J. Luine

Citation: **83**, (1998); doi: 10.1063/1.366925

View online: <http://dx.doi.org/10.1063/1.366925>

View Table of Contents: <http://aip.scitation.org/toc/jap/83/4>

Published by the [American Institute of Physics](#)

Thermal expansion of LaAlO_3 and $(\text{La,Sr})(\text{Al,Ta})\text{O}_3$, substrate materials for superconducting thin-film device applications

B. C. Chakoumakos^{a)}

Solid State Division, Oak Ridge National Laboratory, Oak Ridge, Tennessee 37831-6393

D. G. Schlom

Department of Materials Science and Engineering, Pennsylvania State University, University Park, Pennsylvania 16802-5005

M. Urbanik

Commercial Crystal Laboratories, Inc., 4406 Arnold Avenue, Naples, Florida 33942

J. Luine

TRW, One Space Park, Redondo Beach, California 90278

(Received 7 October 1997; accepted for publication 7 November 1997)

The thermal expansion for the perovskite $(\text{La,Sr})(\text{Al,Ta})\text{O}_3$, i.e., LSAT, grown from the formulation $0.29(\text{LaAlO}_3):0.35(\text{Sr}_2\text{AlTaO}_6)$, was determined by Rietveld refinement of neutron powder diffraction data over the temperature range of 15–1200 K. In comparison to LaAlO_3 the relative volume thermal expansion is the same, although the cell volume of LSAT is slightly larger. Site occupation refinement for LSAT gives a structural formula of $(\text{La}_{0.29(5)}\text{Sr}_{0.71(5)})_{\text{A site}}(\text{Al}_{0.65(1)}\text{Ta}_{0.35(1)})_{\text{B site}}\text{O}_3$. At and below 150 K, LSAT shows a small distortion from cubic symmetry. Unlike the cubic-to-rhombohedral transition (800 K) observed in LaAlO_3 , the low temperature structural phase transition in LSAT appears to be cubic-to-tetragonal or cubic-to-orthorhombic. The rms displacement of the A site in LSAT is significantly larger than that for LaAlO_3 , and about half of the difference can be accounted for by a static displacement component. © 1998 American Institute of Physics. [S0021-8979(98)06904-7]

I. INTRODUCTION

Various oxide perovskites are widely used as single-crystal substrates for epitaxial thin-film growth of the important cuprate superconductors, including $\text{YBa}_2\text{Cu}_3\text{O}_{7-x}$. For this purpose, the ideal substrate should be lattice matched, chemically compatible, thermal expansion matched, and undergo no structural phase transitions between the film growth temperature and the device use temperature.¹ The latter often leads to microtwinning, which can produce deleterious surface roughening and lateral distortions. For microwave device applications, a low permittivity is also desired. To date few, if any, substrate materials offer optimal performance for all of the desired characteristics. Given the rapidly developing application of thin-film cuprate devices for microwave filtering and receiving, it is anticipated that an ideal substrate material will have significant commercial impact. In the course of searching for better oxide perovskites that can be used as commercial substrates for high T_c superconducting thin-film device applications, we have measured the thermal expansion and delineated the structural phase transitions for the title compounds over the temperature range of 15–1273 K by means of neutron powder diffraction.

II. EXPERIMENT

Single-crystals LaAlO_3 were grown by the flame-fusion method (Commercial Crystal, Inc.),² and the

$(\text{La,Sr})(\text{Al,Ta})\text{O}_3$ (LSAT), formulated as $0.29(\text{LaAlO}_3):0.35(\text{Sr}_2\text{AlTaO}_6)$, was grown by the Czochralski method (Lucent Technologies, Inc.). Pieces of the crystals were powdered in an automatic mortar.

Neutron-diffraction data were collected using the HB-4 high-resolution powder diffractometer at the High-Flux Isotope Reactor at Oak Ridge National Laboratory. This instrument has a seven-element vertically focusing Ge (115) monochromator. The Ge crystal segments for this mechanism were precision cut with very low kerf loss using specialized gang saws at Commercial Crystals, Inc. With a monochromator $2\theta=87^\circ$, the 117 and 115 reflections were used to give neutrons with wavelengths of 1.0911(2) Å and 1.4997(1) Å, respectively, calibrated with a Si standard. Soler slit collimators of 12 and 20' are positioned before and after the monochromator crystal, respectively. An array of 32 nearly equally spaced (2.7°) ³He detectors, each with a 6' mylar foil collimator, was step scanned (0.05°) over a range of 40° for scattering angles between 11° and 135°. The samples were sealed in vanadium cans (9 mm by 5 cm) with He exchange gas for data collection from 10 to 350 K using a closed-cycle He refrigerator. For the high temperature measurements, vanadium cans with loose fitting boron nitride ceramic lids were used in a vacuum furnace with a niobium foil heating element encircling the entire sample can. The furnace employed W/Re thermocouples, and sample temperature was externally calibrated by measuring the volume expansion of MgO under the same experimental conditions. For these data collections, the detector array was scanned in

^{a)}Electronic mail: kou@ornl.gov

two segments to overlap up to eight detectors in the middle of the pattern. Overlapping detectors for a given step serves to average the counting efficiency and the two-theta zero-point shift for each detector. Input for the Rietveld refinement program was prepared by interpolating a constant step-size data set from the raw data, because the spacing between the detectors is not exactly the same. The data were also corrected for the variation in detector counting efficiencies, which were determined using a vanadium standard.

Structure refinements were made by the Rietveld method³ using the GSAS software.⁴ The 110 reflection from the Nb heating element of the furnace was observed, and excluded. The pseudo-Voigt peak-profile function truncated at 0.3% of the peak height was used, including six terms.^{5,6} The background was defined by a cosine Fourier series with three to five terms. The coherent scattering lengths used were: La (8.27 fm), Sr (7.02 fm), Al (3.449 fm), Ta (6.91 fm), and O (5.805 fm).⁷

III. RESULTS

For the 300 K LSAT data, the occupations of the A and B sites were refined, giving the structural formula $\text{La}_{0.29(5)}\text{Sr}_{0.71(5)}\text{Al}_{0.65(1)}\text{Ta}_{0.35(1)}\text{O}_3$, which is in excellent agreement with that given by Mateika *et al.*,⁸ $\text{La}_{0.289}\text{Sr}_{0.709}\text{Al}_{0.646}\text{Ta}_{0.356}\text{O}_3$. In the site refinement, no requirement of charge balance is imposed; it relies only on the differences in the scattering length between La and Sr and Al and Ta to match the overall intensity distribution of the pattern. That the refinement result gives charge neutrality is satisfying. For the refinements at other temperatures, the metal sites were held fixed.

For LaAlO_3 , the well-established and studied structural phase transition from rhombohedral-to-cubic occurs at 800 K.⁹ Similarly, we find that at and below 150 K the crystal symmetry of LSAT is also lower than cubic. This distortion of the crystal lattice is evidenced by extra weak reflections which grow as the temperature is lowered (Fig. 1). The data for temperatures at and below 150 K are better fit by either the tetragonal model, $I4/mcm$, or the orthorhombic model, $Imma$, with a small orthorhombicity. Both the tetragonal and orthorhombic models fit the low T data equally well, but refinements for the latter were not stable, i.e., all of the least-squares variables could not be released together without the refinement diverging. Higher resolution neutron diffraction data would help to resolve the symmetries of small distortions such as these. For the Rietveld refinements of LSAT, the χ^2 values were between 1.34 and 1.55, and for LaAlO_3 $\chi^2 = 1.21 - 1.88$. Examples of the refined structural data for each of the distinct crystal symmetries, including both structural models for LSAT at low T , are given in Table I.

For both LaAlO_3 and LSAT volume discontinuities are not apparent across the structural phase transitions because they involve only small rotations of essentially rigid octahedra. Both materials exhibit nearly the same relative volume thermal expansion (Fig. 2), although the cell for LSAT is slightly larger than that of LaAlO_3 . For LaAlO_3 least-squares analysis of the temperature dependence of the lattice parameters for the hexagonal portion (10–800 K) gives the follow-

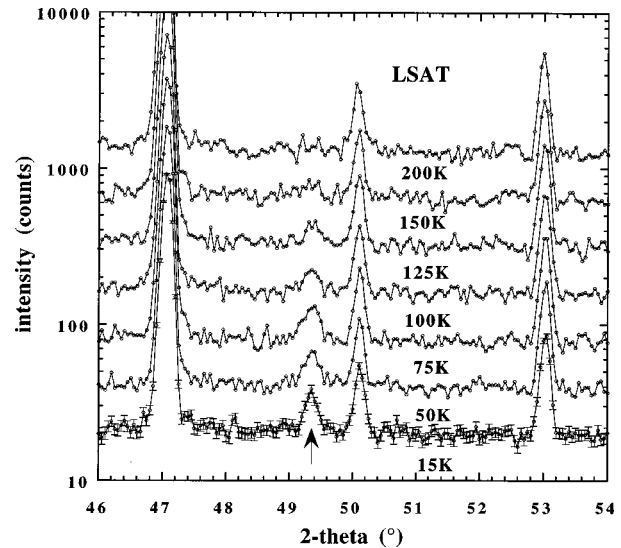


FIG. 1. Neutron powder diffraction patterns ($\lambda = 1.0913 \text{ \AA}$) for LSAT as a function temperature. The weak reflection indicated by the arrow grows as the temperature decreases indicates a reduction from cubic symmetry. The patterns are offset along the y axis for clarity, and the 15 K data shows typical counting errors.

ing: $a = 5.3597 + 4.928 \times 10^{-7} T + 6.032 \times 10^{-8} T^2 - 2.117 \times 10^{-11} T^3 \text{ \AA}$, $c = 13.085 + 3.099 \times 10^{-5} T + 2.012 \times 10^{-7} T^2 - 8.883 \times 10^{-11} T^3 \text{ \AA}$, where T is in K. The volume fit over the entire T interval (15–1230 K) is $V = 54.245 + 2.527 \times 10^{-4} T + 1.747 \times 10^{-6} T^2 - 5.885 \times 10^{-10} T^3 \text{ \AA}^3$. For LSAT, the least-squares fits are: $V = 57.633 + 3.913 \times 10^{-4} T + 1.750 \times 10^{-6} T^2 - 6.514 \times 10^{-10} T^3 \text{ \AA}^3$ over the

TABLE I. Crystal structure data for LaAlO_3 and LSAT.

LaAlO_3				
1223 K, $Pm\bar{3}m$, $a = 3.82842(6) \text{ \AA}$				
atom	x	y	z	$U_{\text{iso}}(\text{Å}^2)$
La	1/2	1/2	1/2	0.0141(3)
Al	0	0	0	0.0126(6)
O	1/2	0	0	0.0216(2)
296 K, $R\bar{3}c$, $a = 5.36462(4) \text{ \AA}$, $c = 13.1096(1) \text{ \AA}$				
atom	x	y	z	$U_{\text{iso}}(\text{Å}^2)$
La	0	0	0	0.0045(3)
Al	0	0	1/4	0.0021(1)
O	0.47505(8)	0	1/4	0.0052(1)
$(\text{La}_{0.29(5)}\text{Sr}_{0.71(5)})_A(\text{Al}_{0.65(1)}\text{Ta}_{0.35(1)})_B\text{O}_3$				
1179 K, $Pm\bar{3}m$, $a = 3.9735(1) \text{ \AA}$				
atom	x	y	z	$U_{\text{iso}}(\text{Å}^2)$
A	1/2	1/2	1/2	0.0229(4)
B	0	0	0	0.0093(4)
O	1/2	0	0	0.0201(6)
15 K, $I4/mcm$, $a = 5.4631(2) \text{ \AA}$, $c = 7.7271(6) \text{ \AA}$				
atom	x	y	z	$U_{\text{iso}}(\text{Å}^2)$
A	0	1/2	1/4	0.0063(1)
B	0	0	0	0.0023(3)
O1	0.2394(1)	0.7394	1/4	0.0069(3)
O2	0	0	1/4	-0.0010(4)
15 K, $Imma$, $a = 5.4620(3) \text{ \AA}$, $b = 7.7279(4) \text{ \AA}$, $c = 5.4635(4) \text{ \AA}$				
atom	x	y	z	$U_{\text{iso}}(\text{Å}^2)$
A	0	1/4	0.001(1)	0.0063(1)
B	0	0	1/2	0.0023(3)
O1	0	1/4	0.516(1)	0.0108(7)
O2	1/4	0.0058(7)	1/4	0.0011(2)

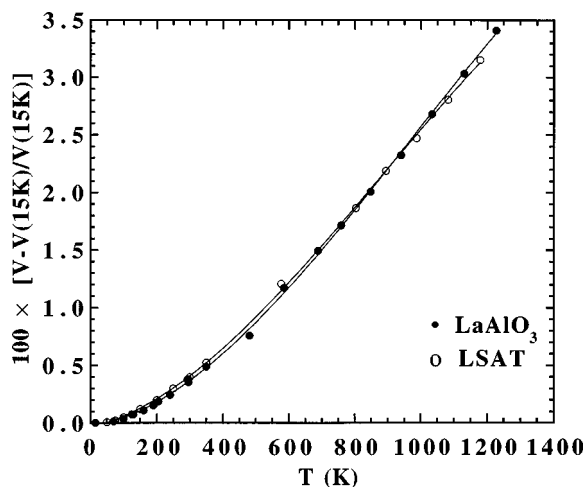


FIG. 2. Relative volume thermal expansion of $(\text{La,Sr})(\text{Al,Ta})\text{O}_3$ and LaAlO_3 .

entire T interval (15–1200 K), and for the cubic region $a = 3.8603 + 2.246 \times 10^{-5} T + 1.783 \times 10^{-8} T^2 - 5.076 \times 10^{-12} T^3$ Å.

The isotropic atomic displacement parameters for the A , B , and O sites exhibit linear behavior in the high temperature region (Fig. 3), as expected from the general form of $U(T)$.¹⁰ The temperature dependences of U for both the O and the B sites are essentially the same for both materials; however, there is more scatter in the latter. For the A site, both the slope of $U(T)$ and the rms displacement are larger for LSAT than for LaAlO_3 . It may be possible to empirically relate the slope and magnitude of $U(T)$ with factors such as coordination number, formal valence, site symmetry, polyhedral volume, bond valence sum, electronegativity, atomic number, Debye temperature, phonon density of states, or atomic size;¹¹ but it is premature to attempt this now as a large number of systematic studies are first required. Never-

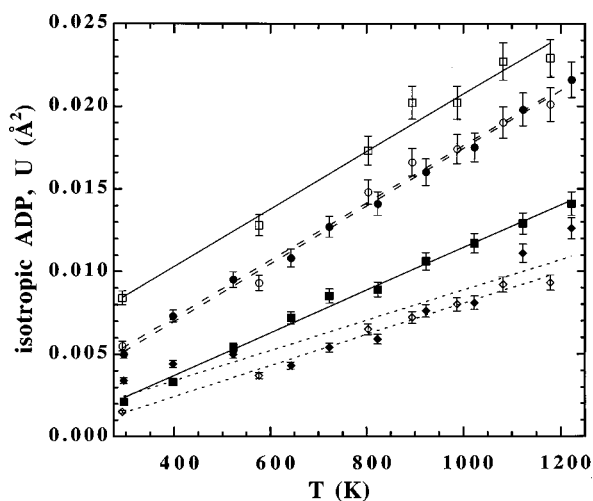


FIG. 3. Temperature dependence of the isotropic atomic displacement parameters for the A (square symbols), B (diamond symbols), and O sites (circle symbols) of $(\text{La,Sr})(\text{Al,Ta})\text{O}_3$ (open symbols) and LaAlO_3 (solid symbols). The lines are least-squares fits for the high temperature portion shown.

theless, further analysis is possible to separate the static positional disorder from the dynamic thermal motion. Using the inequality derived by Housley and Hess,¹²

$$U_j^2(0) \leq U_j(T) h^2 / (16 \pi^2 m_j K_B T), \quad (1)$$

where h = Planck constant, K_B = Boltzmann constant, m_j = the mass of atom j , and T is the temperature in Kelvins, an estimate of the maximum thermal contribution to $U(0)$ can be made by extrapolating (1) to high T where it approaches an equality; see examples given by Cheary¹³ and Argyriou.¹⁴ Assuming that $U_j = U_j^{\text{thermal}} + U_j^{\text{static}}$, the minimum static contribution to U_j can be estimated by subtracting the maximum thermal contribution from the lowest temperature measurement, which in this study is 15 K. When this analysis is applied to LSAT and LaAlO_3 , only the A site of LSAT is indicated to have any static disorder, amounting to 0.0025 \AA^2 , whereas all of the other atomic displacement parameters are explained by thermal vibration alone.

IV. SUMMARY

In the Rietveld refinements of neutron powder diffraction data, unconstrained site refinements for LSAT confirm the expected nominal composition. From 1200 K to just above 150 K, LSAT has cubic symmetry. Below 150 K, the crystal symmetry of LSAT is lower than cubic. The powder diffraction data for temperatures at and below 150 K are better fit by either the tetragonal model, $I4/mcm$, or the orthorhombic model, $Imma$, with a small orthorhombicity. For both LaAlO_3 and LSAT, volume discontinuities are not apparent across the structural phase transitions because they involve only small rotations of essentially rigid octahedra. Both materials exhibit nearly the same relative volume thermal expansion, but the cell volume for LSAT is slightly larger. The rms displacement of the A site in LSAT is significantly larger than that for LaAlO_3 and about half of the difference can be accounted for by a static displacement component.

ACKNOWLEDGMENTS

Brent Taylor, Ron Maples, and Dan Glandon provided invaluable technical assistance with the vacuum furnace. Oak Ridge National Laboratory is managed by Lockheed Martin Energy Research Corporation for the U.S. Department of Energy under Contract No. DE-AC05-96OR22464.

¹J. M. Phillips, *Mater. Res. Bull.* **20**, 35 (1995); J. M. Phillips, *J. Appl. Phys.* **79**, 1828 (1996).

²R. W. Simon, C. E. Platt, A. E. Lee, G. S. Lee, K. P. Daly, M. S. Wire, J. A. Luine, and M. Urbanik, *Appl. Phys. Lett.* **53**, 2677 (1988).

³H. M. Rietveld, *J. Appl. Crystallogr.* **2**, 65 (1969).

⁴A. C. Larson and R. B. Von Dreele, *GSAS—General Structure Analysis System*. Report LA-UR-86-748, Los Alamos National Laboratory, Los Alamos, NM 87545, 1990.

⁵P. Thompson, D. E. Cox, and J. B. Hastings, *J. Appl. Crystallogr.* **20**, 79 (1987).

⁶R. B. Von Dreele, in *Modern Powder Diffraction*, edited by D. L. Bish and J. E. Post (Mineralogical Society of America, Washington, 1989), pp. 333–369.

⁷V. F. Sears, *Neutron News* **3**, 26 (1992).

⁸D. Mateika, H. Kohler, H. Laudén, and E. Völkel, *J. Cryst. Growth* **109**, 447 (1991).

- ⁹H. M. O'Bryan, P. K. Gallagher, G. W. Berkstresser, and C. D. Brandle, *J. Mater. Res.* **5**, 183 (1990); H. Fay and C. D. Brandle, *J. Appl. Phys.* **38**, 3405 (1967); K. A. Müller, W. Berlinger, and F. Waldner, *Phys. Rev. Lett.* **21**, 814 (1968); S. Geller and P. M. Racciah, *Phys. Rev. B* **2**, 1167 (1970).
- ¹⁰B. T. M. Willis and A. W. Pryor, *Thermal Vibrations in Crystallography* (Cambridge University Press, Cambridge, 1975).
- ¹¹B. C. Chakoumakos, *Physica B* (in press).
- ¹²R. M. Housley and F. Hess, *Phys. Rev.* **146**, 517 (1966).
- ¹³R. W. Cheary, *Acta Cryst. Sect. B* **47**, 325 (1991).
- ¹⁴D. N. Argyriou, *J. Appl. Crystallogr.* **27**, 155 (1994).